Influence of convection on the water isotopic composition of the tropical tropopause layer and tropical stratosphere

10 authors, including:

Thomas F Hanisco
NASA
115 PUBLICATIONS **2,476** CITATIONS

E. J. Moyer
University of Chicago
94 PUBLICATIONS **1,437** CITATIONS

Jessica Smith
Harvard University
82 PUBLICATIONS **1,065** CITATIONS

Mark Francis Witinski
Pendar Technologies
28 PUBLICATIONS **175** CITATIONS

Some of the authors of this publication are also working on these related projects:

Project   Infrared Gas Measurements View project

Project   Open Path Gas Detection View project

Influence of convection on the water isotopic composition of the tropical tropopause layer and tropical stratosphere

D. S. Sayres,[1] L. Pfister,[2] T. F. Hanisco,[1,3] E. J. Moyer,[1,4] J. B. Smith,[1] J. M. St. Clair,[1,5] A. S. O'Brien,[1] M. F. Witinski,[1] M. Legg,[6] and J. G. Anderson[1]

[1] We present the first in situ measurements of HDO across the tropical tropopause, obtained by the integrated cavity output spectroscopy (ICOS) and Hoxotope water isotope instruments during the Costa Rica Aura Validation Experiment (CR-AVE) and Tropical Composition, Cloud and Climate Coupling (TC4) aircraft campaigns out of Costa Rica in winter and summer, respectively. We use these data to explore the role convection plays in delivering water to the tropical tropopause layer (TTL) and stratosphere. We find that isotopic ratios within the TTL are inconsistent with gradual ascent and dehydration by in-situ cirrus formation and suggest that convective ice lofting and evaporation play a strong role throughout the TTL. We use a convective influence model and a simple parameterized model of dehydration along back trajectories to demonstrate that the convective injection of isotopically heavy water can account for the predominant isotopic profile in the TTL. Air parcels with significantly enhanced water vapor and isotopic composition can be linked via trajectory analysis to specific convective events in the Western Tropical Pacific, Southern Pacific Ocean, and South America. Using a simple model of dehydration and hydration along trajectories we show that convection during the summertime TC4 campaign moistened the upper part of the TTL by as much as 2.0 ppmv water vapor. The results suggest that deep convection is significant for the moisture budget of the tropical near-tropopause region and must be included to fully model the dynamics and chemistry of the TTL and lower stratosphere.

Citation: Sayres, D. S., L. Pfister, T. F. Hanisco, E. J. Moyer, J. B. Smith, J. M. St. Clair, A. S. O'Brien, M. F. Witinski, M. Legg, and J. G. Anderson (2010), Influence of convection on the water isotopic composition of the tropical tropopause layer and tropical stratosphere, *J. Geophys. Res.*, *115*, D00J20, doi:10.1029/2009JD013100.

1. Introduction

[2] Water vapor and ice exert a controlling influence on the radiative and dynamical balance of the upper troposphere and lower stratosphere (UT/LS) and are key constituents in determining this region's response to climate forcing [*Smith et al.*, 2001; *Fasullo and Sun*, 2001; *Minschwaner and Dessler*, 2004]. The concentration of water vapor in the stratosphere also impacts the dosage of UV radiation reaching the surface through water's control of heterogeneous stratospheric ozone depletion [*Dvortsov*

and Solomon, 2001; *Kirk-Davidoff et al.*, 1999]. In the UT/LS water vapor concentrations are central to the formation, evolution, and lifetime of cirrus that not only play a critical role in the radiative balance in the UT/LS but also in the dehydration of air ascending through the tropical tropopause layer (TTL). Changes in water vapor concentrations and the cirrus associated therewith control the radiative imbalance that amplifies climate forcing by carbon dioxide and methane release at the surface and therefore quantifying the mechanisms that control water vapor in the TTL are key to predicting future changes in the climate system.

[3] Quantifying the importance of convection in transporting boundary layer air to the TTL (for the purposes of this paper defined as the region between 360 K and 380 K theta surfaces) and lowermost stratosphere is pivotal for understanding the mechanisms that control the stratospheric water vapor budget and accordingly that of other trace gases and particulates. Due to this importance much emphasis has been placed on understanding the mechanisms that control the water vapor budget of the TTL and UT/LS. In general, water vapor in the TTL is removed by in-situ condensation and cirrus formation on cooling during ascent or advection

---
[1]School of Engineering and Applied Sciences, Harvard University, Cambridge, Massachusetts, USA.
[2]NASA Ames Research Center, Moffett Field, California, USA.
[3]Now at NASA Goddard Space Flight Center, Greenbelt, Maryland, USA.
[4]Now at Department of Geophysical Sciences, University of Chicago, Chicago, Illinois, USA.
[5]Now at Geology and Planetary Sciences Division, California Institute of Technology, Pasadena, California, USA.
[6]BAERI, Sonoma, California, USA.

through local cold regions [*Holton et al.*, 1995; *Holton and Gettelman*, 2001; *Fueglistaler et al.*, 2005]. Convection can however provide additional sources of water via evaporation of convective ice in undersaturated TTL air [*Fu et al.*, 2006; *Hanisco et al.*, 2007; *Dessler et al.*, 2007]. Distinguishing the importance of the relevant mechanisms will allow models to better simulate how water vapor pathways linking the troposphere and stratosphere will change with increased climate forcing by carbon dioxide and methane. Many modeling studies that attempt to reproduce the observed water vapor mixing ratio of the TTL have suggested that convective ice lofting and evaporation may be unimportant to the region's water budget, and that mixing ratios of water vapor in air crossing the tropical tropopause can be well explained simply by the minimum temperature experienced by those air parcels [*Fueglistaler et al.*, 2004, 2005; *Gulstad and Isaksen*, 2007; *Cau et al.*, 2007]. However, attempts to simultaneously model HDO mixing ratios find that convection is necessary to accurately reproduce observed profiles of both H_2O and HDO [*Dessler et al.*, 2007; *Bony et al.*, 2008]. Because water vapor isotopic composition is altered by all processes involving condensation or evaporation, the ratio of water vapor isotopologues (HDO/H_2O or $H_2^{18}O$/H_2O) can act as a tracer of an air parcel's convective history [*Pollock et al.*, 1980; *Moyer et al.*, 1996; *Keith*, 2000]. Therefore, adding HDO to models constrains the amount of convection allowable and necessary in the model. Any model that attempts to explain the water vapor mixing ratio must also explain the water vapor isotopologue ratio which is usually written as the ratio of the heavier isotope (e.g. HDO or $H_2^{18}O$) to the more abundant lighter isotope (H_2O) referenced to a standard. In the case of water the reference is the ratio in Vienna Standard Mean Ocean Water (R_{VSMOW}) [*Craig*, 1961a]. Deviations from the standard, δ, are reported in permil (‰) where for the HDO/H_2O ratio $\delta D = 1000(HDO/H_2O/R_{VSMOW} - 1)$. Values of $\delta D \approx -80‰$ are found close to the boundary layer and more negative values (e.g. $\delta D = -600‰$) are found in highly dehydrated air masses near the tropopause.

[4] Measurements of δD from canisters and remote observations have reported enriched values of HDO compared to what would be expected from simple thermally controlled dehydration mechanisms [*Moyer et al.*, 1996; *Johnson et al.*, 2001; *Kuang et al.*, 2003; *Ehhalt et al.*, 2005]. To try to better model the observed δD ratio [*Dessler et al.*, 2007], hereafter Dessler07, used the *Fueglistaler et al.* [2005] trajectory model and added a climatological representation of convective ice flux to demonstrate that addition of water from evaporating convective ice was indeed a plausible explanation for isotopic enhancements observed by remote sensing instruments. Dessler07 were able to reproduce the δD profile from remote observations with only a small perturbation to the water vapor mixing ratio produced from the *Fueglistaler et al.* [2005] model.

[5] In this paper we present the first in situ tropical measurements of HDO obtained during both winter and summer. The high spatial and temporal resolution of the in situ data offer a more detailed test case than did the relatively coarse remote sensing data used by Dessler07. The in situ data are tied directly to diabatic back trajectories from the point of the measurement to identify sources of recent convective influence and to quantify the effect of convection

on the δD ratio and the water vapor mixing ratio. We then apply our own convective influence scheme, which uses real-time convection observations as opposed to the climatology employed by Dessler07, to evaluate whether a measurable difference in δD and water vapor mixing ratio is observed between data recently influenced by convection. Finally, we simulate the motion of air parcels along trajectories, tracking both water vapor and HDO in order to test if our model reproduces the profiles from the in situ data.

2. Measurements

[6] Isotopologue ratios were measured in situ aboard NASA's WB-57 high-altitude research aircraft during the Costa Rice Aura Validation Experiment (CR-AVE) in January and February, 2006 and the Tropical Composition, Cloud and Climate Coupling (TC4) campaign in August, 2007, both based out of Alajuela, Costa Rica, at 9.9° North latitude. Measurements of H_2O, HDO, and $H_2^{18}O$ were obtained during these campaigns using the Harvard ICOS isotope instrument [*Sayres et al.*, 2009]. We focus here primarily on HDO which, although less abundant than $H_2^{18}O$, experiences stronger fractionation on condensation, giving the isotope ratio observations more robustness against any instrument systematics. For TC4, H_2O and HDO measurements were also obtained by the total water Hoxotope instrument [*St. Clair et al.*, 2008]. Water vapor mixing ratios are reported using the Harvard Lyman-α hygrometer [*Weinstock et al.*, 1994], which has a long heritage on the WB-57 aircraft.

[7] Data reported here are screened for both potential contamination and potential instrument systematics. To preclude inclusion of any ICOS data subject to contamination from water desorbing off the instrument walls, we report only ICOS data where ICOS water vapor is less than 0.5 ppmv greater than that reported by Harvard Lyman-α. An additional potential source of measurement uncertainty in the ICOS data is optical fringing and other artifacts in the baseline power curve, which can produce measurement biases that manifest themselves as offsets in measured δD. While fitting routines developed for ICOS (as described by *Sayres et al.* [2009]) mitigate some potential sources of bias, residual offsets on the order of 50‰ to 100‰ are still occasionally present. Periods of high potential bias are however readily identified and for this work we have removed all data with potential biases greater than the short term 1-σ measurement precision. Quality-controlled ICOS data during CR-AVE in the driest, most signal-limited conditions (H_2O < 10 ppmv) show a maximum uncertainty in δD of 17‰ (30 sec., 1-σ). (In wetter air, signal to noise is higher and therefore isotopic ratio uncertainty lower). For the TC4 mission, a laser change in the ICOS instrument resulted in increased bias uncertainty in low-signal conditions. We therefore show here ICOS data from TC4 only for wetter conditions (H_2O > 10 ppmv) and use Hoxotope data for dry conditions or for flights when ICOS did not report data. The base Hoxotope precision is 50‰ (30 sec., 1 σ). Although these uncertainties exceed those of laboratory-based mass spectrometers, they represent the most sensitive in situ water isotope measurements made in these conditions, and are comparable with the performance of remote
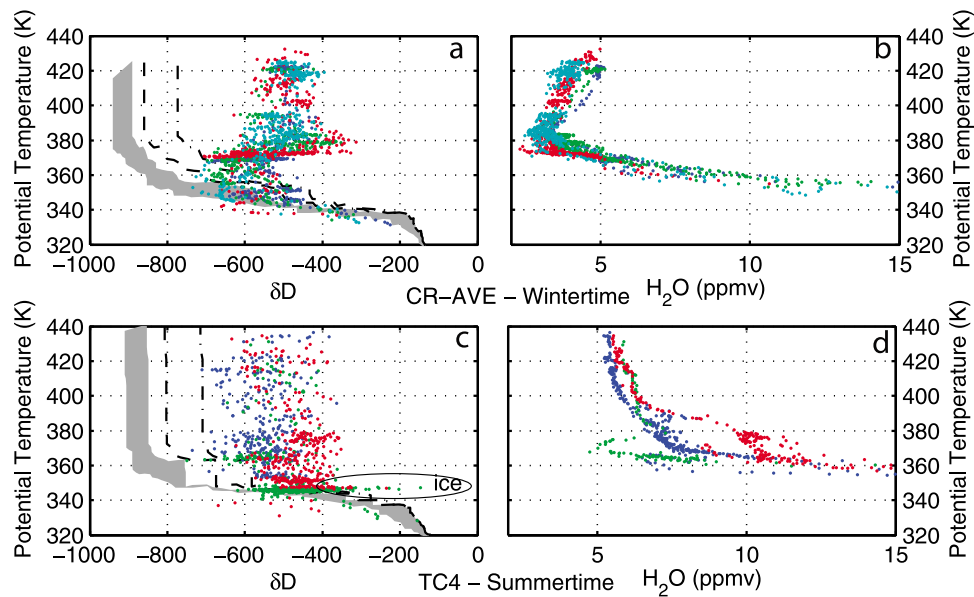
Figure 1. Profiles of (left) δD and (right) water vapor mixing ratio versus potential temperature for flights during (a, b) CR-AVE and (c, d) TC4. For CR-AVE profiles made during the flights of January 30th (blue), February 1st (green), February 2nd(red), and February 7th (cyan) are shown. For TC4 profiles made during the flights of August 6th (blue), August 8th (green), and August 9th (red) are shown. For Figures 1a and 1c the shaded region represents the range of values from a Rayleigh distillation model. The Rayleigh curve plotted here is based on minimum and maximum temperature profiles during each campaign and bounded on the left by an ideal curve where vapor condenses at 100% relative humidity and the condensate is immediately removed and on the right by a curve that includes the effect of 80% condensate retention as the air parcel rises. Retention is important in the liquid phase where re-equilibration can occur. The shift in the Rayleigh curve due to condensation under supersaturated conditions are shown as dashed and dot-dashed black lines for relative humidity of 120% and 150%, respectively.

sensing instruments while providing far higher spatial and temporal resolution.

[8] In order to restrict our analysis to true tropical air masses we show here only data from tropical flight segments out of Alajuela, Costa Rica in which the WB-57 aircraft made vertical transects through the tropopause while in the tropics, i.e. at latitudes below 10° North. Flights with segments meeting both the geographic and data quality criteria in the wintertime (CR-AVE) campaign occurred on January 30, and February 1, 2, and 7, 2006 and in the summertime (TC4) campaign on August 6, 8, and 9, 2007 (Hoxotope) and August 8 and 9, 2007 (ICOS). We include water vapor data from the Lyman-α instrument for all these flight legs.

3. Mean Tropical δD Profiles

[9] The isotopic composition of water vapor in the tropical atmosphere shows a sharp distinction in behavior between the bulk of the troposphere and the TTL (Figure 1). Below the TTL, both water vapor and δD fall off with altitude much as expected in pure Rayleigh distillation, where preferential removal of heavier condensate leaves the residual vapor progressively lighter [*Jouzel et al.*, 1985; *Ehhalt et al.*, 2005]. Within the TTL water vapor concentrations continue to decrease to the tropopause. However, starting below the base of the TTL ($\theta = 340$–360 K) isotopic composition decreases more slowly than expected

if temperature alone were the controlling mechanism and in the TTL δD remains roughly constant. This trend is persistent in both summertime and wintertime observations, but some seasonal difference is evident. The lower part of the TTL is isotopically lighter and drier in the wintertime CR-AVE data (Figures 1a and 1b) with a mean δD of $-650‰$ and minimum water vapor mixing ratio of 2.5 ppmv. The upper part of the TTL, above 370 K, is characterized by an increase in δD to isotopically heavier air with a mean of $-500‰$. This shift is correlated with the slight increase in the water vapor measurements above the tropopause, though the shift in δD starts below the tropopause. In the stratosphere proper, the δD measurements are invariant within the precision limits of the data, while the water vapor mixing ratio increases linearly. During the wintertime there is little variability in the profiles between flights.

[10] In the summertime TC4 data (Figures 1c and 1d), with nearby ITCZ convection, the TTL is isotopically heavier with a mean δD of $-550‰$ and its composition is continuous with the stratosphere proper. The variability is greater in the summertime with noticeable differences between flights. Within the TTL there are three distinct water profiles (Figure 1d). The August 6th profile, plotted in blue, shows typical water vapor mixing ratios for the summertime of about 7 to 8 ppmv. The August 9th profile, plotted in red, is the wettest with mixing ratios around 10 ppmv. The August 8th profile, plotted in green, shows a
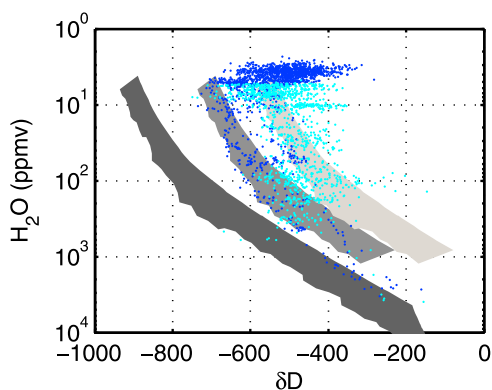
Figure 2. The δD versus water vapor with data from CR-AVE and TC4 shown in blue and cyan, respectively. The shaded regions represent Rayleigh curves (as in Figure 1) with the lighter-gray curves shifted by 200‰ and 350‰ from the dark-gray curve below the base of the TTL.

sharp dip in the middle of the TTL with water vapor mixing ratios as low as 5 ppmv. The δD measurements show similar differences (Figure 1c). The profiles from August 6th and 9th have mean δD values of −550‰ and −450‰, respectively. The δD values from August 8th are isotopically depleted compared to the other flights with a mean of −600‰. Above the TTL there are two distinct profiles. The profile from August 6th is the drier of the two with a minimum at 410 K of 5.5 ppmv. The second profile was sampled on both August 8th and 9th with a mean at 410 K of 6 ppmv. Similar to the TTL, the δD profiles are isotopically depleted for the drier profile and enriched for the moister profile.

[11] As noted in the introduction, observations of isotopically heavy water vapor within the TTL are incompatible with simple dehydration during gradual ascent, which would produce significantly more isotopic depletion along with dehydration. In the bulk of the troposphere, from the lowest observations to a θ of 345 K in the summertime (Figure 1c) and 355 K in the wintertime (Figure 1a), observed water isotopic composition is roughly consistent with a Rayleigh distillation model. Water vapor concentrations fall by over two orders of magnitude and isotopic composition drops to approximately −500‰ and −600‰, in the summertime and wintertime, respectively. Within the TTL, however, observed near-constant isotopic composition cannot be explained by a simple Rayleigh distillation model. Modeled Rayleigh calculations are shown for comparison in Figures 1a and 1c (gray shaded region; see caption for model parameters). Gradual ascent and pure Rayleigh distillation within the TTL would further reduce vapor isotopic composition to a δD of −900‰ as opposed to the observed δD values between −400‰ and −650‰. In the stratosphere proper, we would expect no further change save a slight increase due to methane oxidation as air ages. To within the precision of the data, δD is indeed invariant above the tropopause; the aircraft flights do not sample high enough altitudes or old enough air ages for methane oxidation to be significant.

[12] Thus far we have evaluated the water vapor and δD measurements separately even though when in equilibrium they follow a very tight relationship that can be seen by

plotting the logarithm of the water vapor mixing ratio versus δD (Figure 2). As shown in Figure 1 the data are isotopically heavy compared to a simple Rayleigh model (dark-gray shaded region). The difference between the Rayleigh model and the data is slightly different in Figures 1 and 2 due to the difference in using potential temperature versus water vapor as the altitude proxy. The Rayleigh relationship modeled here assumes that the air parcels sampled followed a single Rayleigh distillation curve given by the average temperature profile measured by the WB-57 out of Costa Rica. Even if this temperature profile is representative of the tropics, ice evaporation in the free troposphere or lower part of the TTL would have the effect of shifting the Rayleigh curve. As an example, if the Rayleigh curve is shifted by 200‰ or 350‰ below the TTL, the subsequent relationship between water vapor and δD would follow the two lighter-gray shaded regions shown in Figure 2. The CR-AVE data and most of the TC4 data greater than 10 ppmv water vapor fall on these shifted curves indicating that convection at or below the base of the TTL is important for setting the δD value at the base of the TTL. Below 10 ppmv water vapor most of the TC4 data are consistent with the shifted Rayleigh curves, while the CR-AVE data show an additional shift to isotopically heavier values. The enrichment at the base of the TTL may be due to convective ice evaporation in the mid-troposphere, more likely in summertime. In the wintertime that enrichment may have taken place in a different part of the tropics or perhaps even reflect an influx of midlatitude air [*Hanisco et al.*, 2007; *James and Legras*, 2009].

[13] One other possible mechanism that would shift the Rayleigh curve is ice formation under supersaturated conditions. When ice forms under these conditions, kinetic effects between the isotopologues dominate over the thermodynamics with the result that δD is shifted to less depleted values as shown in Figure 1 by the dashed black lines representing condensation at 120% and 150% relative humidity over ice.

[14] Whether condensation at high supersaturation is a major factor in determining the δD ratio can be evaluated by looking at the relationship between δD and δ^{18}O. If condensation follows a Rayleigh process (i.e. is in thermodynamic equilibrium) then the slope of the δD to δ^{18}O relationship follows the well known meteoric water line (MWL) (Figure 3, thick black curved line) [*Craig*, 1961b]. As the level of supersaturation increases, the heavier $H_2^{18}O$ isotopologue is less depleted relative to HDO resulting in the slope between δD and δ^{18}O becoming shallower as shown by the dashed lines in Figure 3. Data falling below the MWL can occur from mixing between parcels with δ ratios at different points along the MWL. Data from CR-AVE and TC4 are plotted in blue and cyan respectively, and while some data indicate condensation under supersaturated conditions, most lie either on the MWL or below in the mixed region. We therefore conclude that condensation at high supersaturation is not a major factor controlling the shift in δD away from the Rayleigh curve and leaves convective ice lofting and subsequent evaporation as the sole possible mechanism for the observed enhancements in δD. This is in agreement with the conclusions of *Keith* [2000] and *Johnson et al.* [2001].

[15] To better quantify the effect of convection within the TTL on δD and water vapor mixing ratio, we conduct two
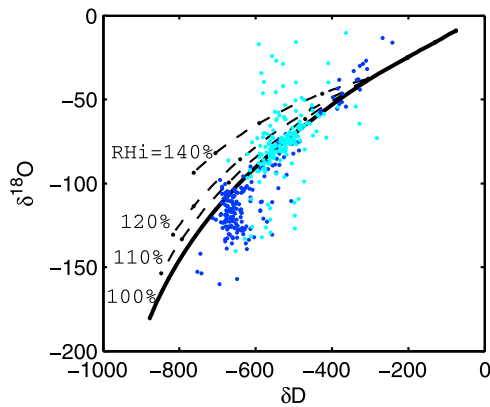
Figure 3. The $\delta^{18}O$ versus δD with data from CR-AVE and TC4 shown in blue and cyan, respectively. Thick black line represents the meteoric water line with the dashed lines showing the effect of supersaturation on the relationship between $\delta^{18}O$ and δD. Points below the meteoric water line result from mixing of air parcels with different δ values.

studies. First, we use a back-trajectory model and maps of past convection to qualitatively examine whether isotopically heavy and moister air can be attributed to specific convectively active regions. Second, we model isotopic evolution along those trajectories to quantitatively verify that addition of convective ice can produce the observed enhancements and quantify the amount of water vapor added by convection.

4. Back Trajectories and Convective Influence Model

[16] The high spatial and temporal resolution of the in situ data allow for the use of back trajectory analysis to determine which sampled air parcels have been influenced by recent convective events and evaluate whether convective influence is indeed correlated with isotopic enhancement. We use for this purpose an analysis framework similar to that of *Pfister et al.* [2001] and briefly documented by *Pfister et al.* [2010]. Diabatic back-trajectories are performed along the flight tracks of the WB-57 aircraft using the GSFC trajectory model [*Schoeberl and Sparling*, 1995] driven by the GEOS-4 analysis [*Bloom et al.*, 2005] and radiative heating rates. For the TC4 calculations, we use the mean July clear-sky radiative heating rates from *Rosenfield* [1991]. For CR-AVE, we use mean winter clear-sky radiative heating rates calculated by *Yang et al.* [2010]. For each aircraft point, a cluster of 20 day trajectories are calculated in order to minimize errors from the back-trajectory analysis and also to allow for a gradient in convective influence, as the convective systems in the TTL are narrow and scarce. Each cluster has 15 points at 3 altitudes; 0.5 km above the aircraft level, at the aircraft level, and 0.5 km below the aircraft level. At each level there are 5 points along a line perpendicular to the aircraft flight track, each separated by 0.3 degrees. The trajectories are run along theta surfaces, with the parcels moving across theta surfaces as indicated by the GEOS-4 heating rates. To calculate convective influence, the trajectories are run through a time varying field of satellite brightness temperature, using global geostationary,

8 km resolution, 3 hourly satellite imagery. Convective influence is defined as occurrences along the trajectories where the satellite brightness temperature is less than or equal to the trajectory temperature. Convective encounters are allowed even if the trajectory is as much as 0.25 degrees distant from the cold temperature. While using the cluster of trajectories and allowing for some distance between the trajectory and the cold temperature convection the model may still miss some convective events either because of the temporal resolution of the model or because ice crystals may reach above the cloud top as defined by the cold temperature.
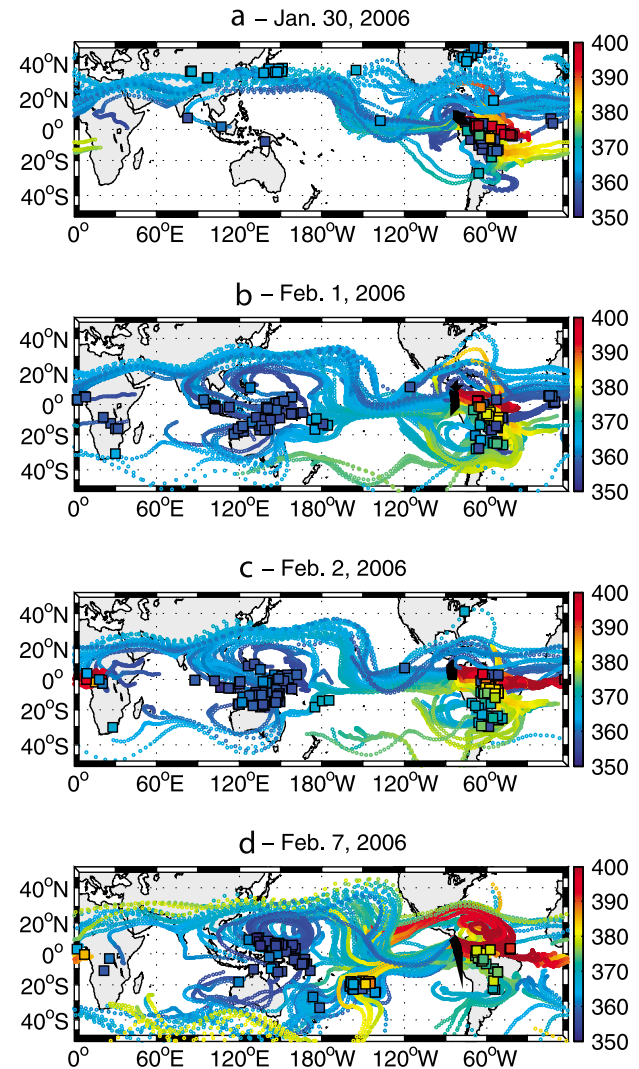

Figure 4. Back-trajectories for flights during the CR-AVE mission. The trajectories start 20 days before the WB-57 sampled the air parcels and end at the point the trajectories intersect the WB-57 flight track, which is shown in black (near 0°–10°N and 80°W). Shown are all trajectories that end above the 355 K isentrope and are colored coded by the potential temperature along the trajectory as given by the colorbar to the right of each plot. Also shown are points along the trajectory where the air was influenced by convection, plotted as black squares also color coded by potential temperature.
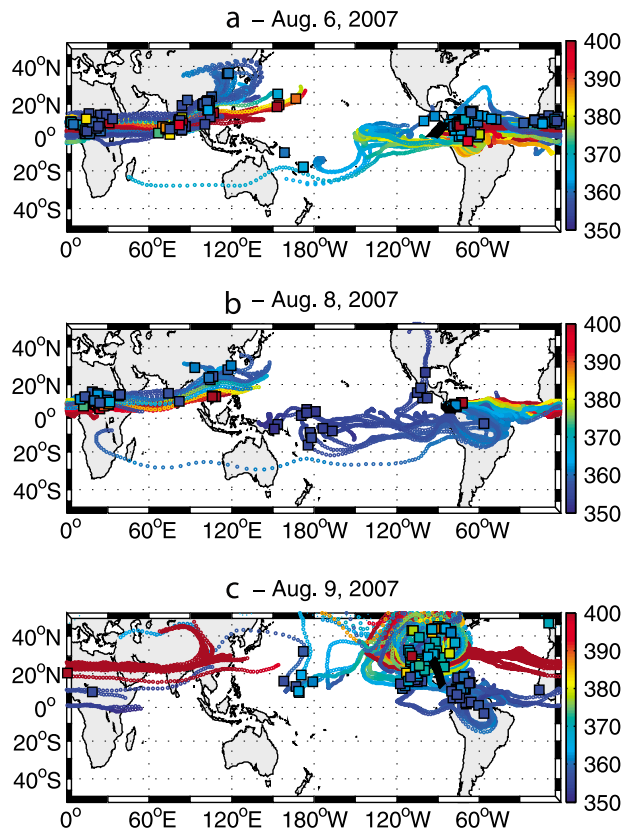
Figure 5. Same as in Figure 4 but for flights during the TC4 mission.

[17] The CR-AVE trajectories (Figure 4) show a clear separation in the origin of the air near the tropopause. Air from the free troposphere and throughout the TTL up to 370 K (colored blue and cyan) mostly originates in the Western Tropical Pacific (WTP) or has circumnavigated the tropics once during the previous 20 days. Some trajectories on February 7th (Figure 4d) also originate from the Southern Pacific Ocean. Air above 370 K (colored green, yellow, and red) has spent most of the previous 20 days over the Caribbean and South America. A few trajectories also follow the tropospheric air that originates from the Southern Pacific and Asia (mostly from the flight of February 7th; see Figure 4d). During CR-AVE deep convection (above $\theta = 380$ K) occurs over South America (Figures 4a, 4b, and 4c), the Southern Pacific Ocean (Figure 4d), and the west coast of Africa (Figures 4c and 4d). The altitude of the shift in origin of air and the observations of deep convection correspond to the shift to isotopically heavier and moister air shown in Figures 1a and 1b. While the air parcels sampled below 370 K were also influenced by convection, this mostly occurred over the WTP at the start of the trajectories. By the time the air was sampled during CR-AVE, most of the water that would have been added by convection may have been removed by desiccation, though the δD values still retain some signature of convective influence. Though convection was not directly measured above the base of the TTL during TC4 or CR-AVE, there is clear observational evidence of convection penetrating above 400 K in the

tropics. *Kelly et al.* [1993] and *Pfister et al.* [1993] noted hydration associated with convection up to 410 K in northern Australia. More recently, *Corti et al.* [2008] have noted hydration up to 420 K, both in Australia and South America.

[18] The tropical trajectories from TC4 (Figures 5a and 5b) originate either from the Asian monsoon region and move westward or from the Southern Pacific Ocean and move eastward. Most of the trajectories have been influenced by convection either over Asia, Africa, or South America. On August 9th (Figure 5c) the WB-57 sampled sub-tropical air originating from the North American monsoon (mid-latitudes). The profiles from August 9th (Figures 1c and 1d, red trace) are heavier and moister, consistent with air from mid-latitudes. The convective influence model also shows significant convection over North America (Figure 5c). The trajectories from August 6th show a higher percentage were influenced by convection as compared with August 8th, with many trajectories influenced recently over South America. This correlates with the difference in water vapor mixing ratio measured on August 6th and 8th (Figure 1d, blue and green traces). Whether the water vapor and δD differences measured during TC4 can be quantitatively attributed to convection and to what extent this convection permanently alters the water vapor mixing ratio will be further explored in the next few sections.

5. Model Description

[19] To help establish whether evaporating convective ice can indeed explain the observed non-Rayleigh isotopic profiles in the tropical TTL, we have added a simulation of isotopic evolution to the back-trajectories and convective influence model described in section 4. We use NCEP reanalysis temperatures [*Kalnay et al.*, 1996], provided by the NOAA/OAR/ESRL PSD (Boulder, Colorado; http://www.esrl.noaa.gov/psd/), to provide initial water vapor and HDO concentrations for the start of each trajectory assuming that the initial water vapor mixing ratio is equal to the saturation mixing ratio. The initial δD is calculated assuming a value of -75‰ in the boundary layer and follows a Rayleigh profile to the altitude at the start of each trajectory. Since this assumption will only be valid in the free troposphere, we restrict our model to trajectories that start below or at the base of the TTL. In order to allow for a representation of mixing in the atmosphere, we run the model along each of the five trajectories at the aircraft altitude from the cluster of trajectories for each aircraft point. As an example, the top map in Figure 6 shows one set of five trajectories. The trajectories follow almost the same path, however one was influenced by convection over Asia, two over Africa (the two squares in Figure 6 overlap), and the last two were not influenced by convection during the previous 20 day period. As the trajectory is run forward, if the air parcel cools the relative humidity is kept equal to 100% and it is assumed that any removal of water by condensation follows Rayleigh distillation and this provides the resultant δD. If the temperature increases and the air becomes undersaturated then the concentration of H_2O and the δD value are left constant unless there is convection. If there is convective influence the model hydrates the air to saturation with evaporated ice that has a δD of -100‰
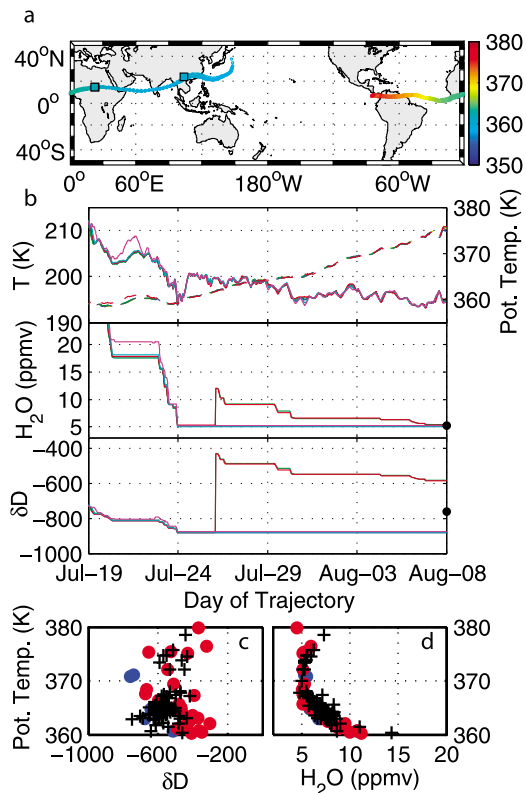
Figure 6. Example of model simulation. (a) The 5 cluster trajectories at the aircraft level color coded by their potential temperature (note the trajectories fall nearly on top of each other). The locations of convective influence are shown as black squares. (b) Temperature, potential temperature, water vapor mixing ratio, and δD of each of the five trajectories plotted versus time along the trajectories (note that the red and green traces and the purple, cyan, and blue traces have nearly the same values). The black points at the end of the trajectories show the mean water vapor mixing ratio and δD of the cluster. (c, d) A sample of the results from the model for all trajectories on a particular day. The model results are shown as colored dots with the in situ data plotted as black crosses.

(see ice data highlighted by Figure 1 and *Hanisco et al.* [2007]). After convection, the air parcel continues along the trajectory as before.

[20] Figure 6b shows the modeled evolution of water vapor mixing ratio and δD for each of the five trajectories. The trajectory that encountered convection over Asia (purple trace) is nearly saturated at the time of possible convective influence and therefore very little effect on water vapor or δD is observed. All five trajectories reach their minimum temperature and therefore their minimum water vapor mixing ratio and δD on July 24th. After that two of the trajectories (red and green traces) encounter convection over Africa with both water vapor and δD increasing sharply. By the end of the trajectories on August 8th the water vapor mixing ratios have decreased to nearly the same value as if they had never encounter convection ($H_2O = 5$ ppmv), but the δD values retain the signature of convection ($\delta D = -600‰$). The mean water vapor mixing ratio and δD for this set of trajectories is show as a black dot. Once the

model has been run for all trajectories it is the mean from each set of cluster trajectories that is compared to the in situ data (Figures 6c and 6d).

6. Sensitivity Analysis

[21] Before comparing the in situ data with the model for all the flights we first evaluate the sensitivity of our model to assumptions about the relative humidity at which water vapor condenses and the initial δD value of the parcel. To quantify the effect of supersaturation on our model results we vary the relative humidity at which condensation occurs between 100% and 180% relative humidity with respect to ice. Once this threshold is reached, water vapor is dehydrated to 100% relative humidity. Shown in Figure 7 are the mean fractional differences between the model results and the in situ data for both water vapor mixing ratio and δD, with a value of zero being perfect agreement. We show the results from three sample flights. Only the water vapor data are used as a metric for determining the best saturation value to use in the model. The δD data are shown for reference as to the effect of higher saturations on δD. August 8th and February 7th are representative of most of the flights from TC4 and CR-AVE. August 6th does not behave in the same manner as the other days and we show it to illustrate the variability observed in the data. On August 8th and February 7th the model results, using a relative humidity of 100% for
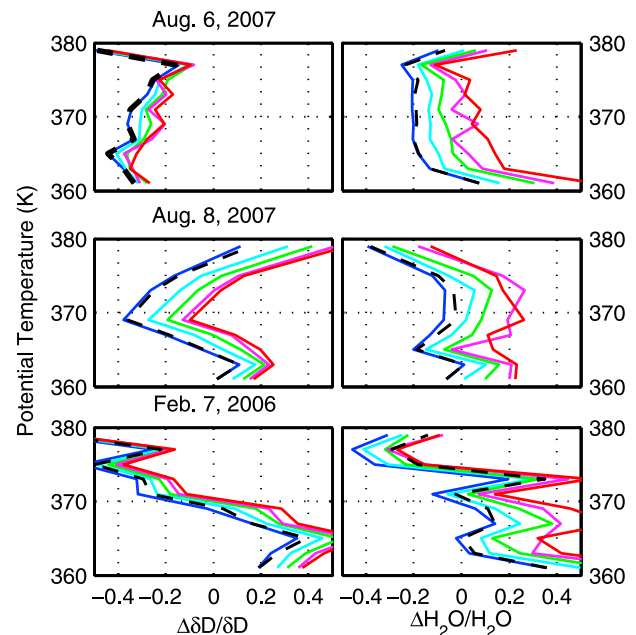

Figure 7. Sensitivity of water vapor mixing ratio and δD from the model to the relative humidity at which condensation occurs for select days. Shown are the fractional differences between the model and the in situ data using a relative humidity required for condensation of 100% (blue), 120% (cyan), 140% (green), 160% (magenta), and 180% (red). Also shown is a temperature dependent relative humidity curve as described in the text (dashed black line). Negative values mean the model results are lower than the in situ data and positive values mean the model results are higher than the in situ data.
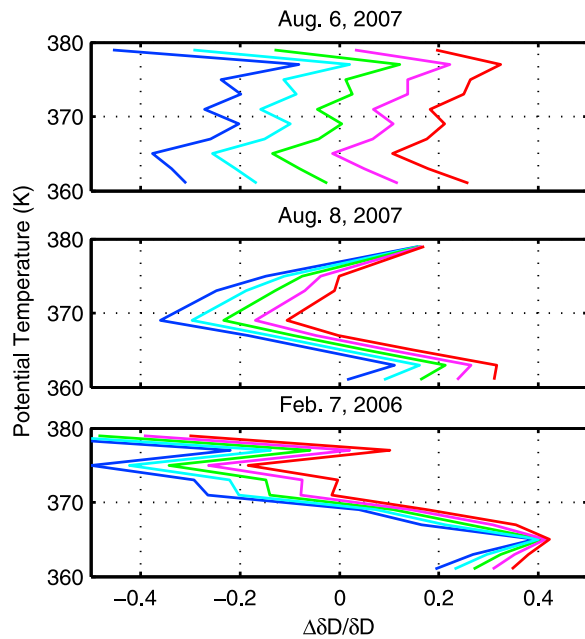
Figure 8. Sensitivity of δD from the model to the initial δD at the start of the trajectory. Shown are the fractional differences between the model and the in situ data for a δD shift of +0‰ (blue), +100‰ (cyan), +200‰ (green), +300‰ (magenta), and +400‰ (red).

the condensation point (blue traces in Figure 7), agree well with the in situ data below a θ of 370 K. Above 370 K higher saturation levels (up to 160–180%, magenta and red traces) are needed to produce better agreement between the data and model. This is not surprising as observations of high supersaturation are common at cold temperatures [*Jensen and Pfister*, 2005; *Jensen et al.*, 2005]. In order to better simulate this dependence on temperature, we use a relative humidity of 100% for temperatures greater than 195 K. For temperatures below 195 K we increase the relative humidity allowed as temperature decreases using a linear interpolation with a relative humidity of 100%, 130%, 180%, and 200% at temperatures of 195K, 190K, 185K, and 180K (based on archived data from tropical missions: CWVCS, Pre-AVE, AVE, CR-AVE, and TC4). This scheme produces overall better agreement in water vapor for both CR-AVE and TC4 throughout the TTL and this is the scheme used for the model results presented in sections 7 and 8. August 6th stands out as in order to achieve agreement between the model and the in situ data a relative humidity of 160% is needed at all temperatures, though in several other days higher supersaturation at the coldest temperatures would produce better results (for example on August 8th above θ of 375 K the red trace gives better agreement than either the blue or dashed-black traces). Whether this is due to the simplicity of our model or real variability in the atmosphere is unclear.

[22] The δD results from the model are also effected by relative humidity as condensation under supersaturated conditions produces less fractionation. δD is also sensitive to the initial assumptions. If we assume that the δD at the start of each trajectory is set by Rayleigh distillation up to that point, then in general the model underestimates the δD

value, especially above a θ of 370 K. However, we know that convection can occur lower down in the troposphere (i.e. before the start of the trajectory) and the signature of that convection will remain. This is in agreement with the observations from CR-AVE and TC4 that show that data below the TTL is shifted from a pure Rayleigh curve (see Figure 2). We perform a sensitivity study allowing the initial value of δD to be increased from its pure Rayleigh value by between 0 and 400‰ (Figure 8). The results of this study show a high level of variability from day to day and with altitude, likely reflecting the high variability of convection in the tropics. To limit the number of parameters in the model we choose a single δD shift using the in situ data to set the shift in δD. For CR-AVE we add 200‰ to the start of each trajectory and for TC4 we add 300‰ to the start of each trajectory.

[23] Due to the long duration of these trajectories (20 days) and that the minimum temperature encountered by the air parcels occurs within those 20 days we find that the model is insensitive to assumptions about the initial water vapor mixing ratio (i.e. that the parcel starts saturated). The other parameter that the model is sensitive to is the δD of the ice. We base the δD of ice in the model on the limited number of observations available. However, it is likely that this value is variable and dependent on a variety of parameters including the amount of air entrained along the convective turret, the location of the convection, and the amount of mixing between the convection and ambient air. Since we do not have sufficient observations to map the variability we fix the δD of ice at 100‰.

7. Model Results From TC4

[24] We use the three flights from the TC4 mission to test whether the temperature histories experienced by the sampled air parcels during the previous 20 days along with the representation of convective influence can accurately reproduce the observed water vapor mixing ratio and δD values. We limit our analysis to the trajectories ending (i.e. the altitude at which the WB-57 sampled the air parcels) in the TTL region with θ between 360 and 380 K. We pick the TTL region both because of the flight to flight variation observed in this region during TC4 and because the use of a Rayleigh model to provide the initial δD values at the start of the trajectory is only reasonable for trajectories that originate below the TTL.

[25] With the assumptions and parameters laid out in sections 5 and 6 the model reproduces the in situ water vapor mixing ratio and δD profiles observed during TC4 (Figure 9). There are several features worth noting. The model correctly reproducing the observed variability in the water vapor profiles during TC4 and also the atmospheric variability within each profile. As shown in Figure 1, three different air masses were sampled with different water vapor mixing ratios and the model quantitatively reproduces those differences. On August 6th and 8th (Figures 9b and 9d) when the in situ data form a very tight profile (i.e. little spread in the data at each altitude) the model results are also tightly correlated. On August 9th (Figure 9f) than the water vapor mixing ratios indicating that the effect of convection is more complicated than the effect of temperature. The agreement tends to be worse in the lower part of the TTL,
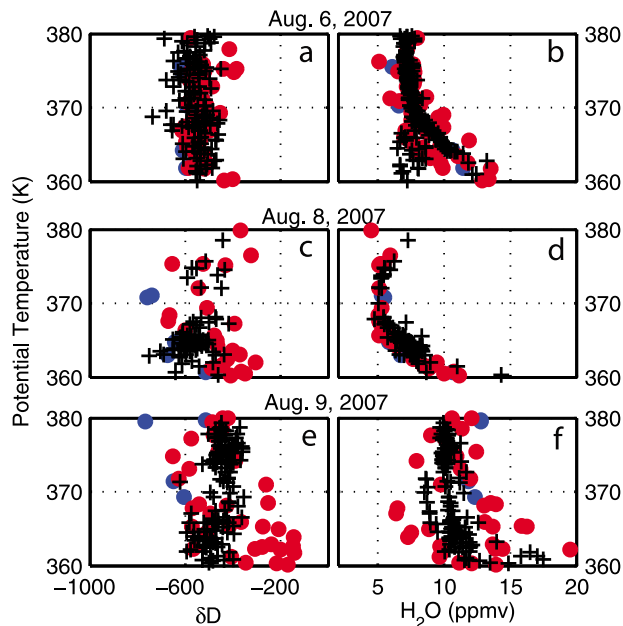
Figure 9. Comparison of model results and in situ data from TC4. Calculated and measured (a, c, e) δD and (b, d, f) water vapor are plotted versus potential temperature. Model results are plotted in blue and red for trajectories that were influenced by convection and those that were not influenced by convection in the past 20 days. The measured mixing ratios and δD are shown as black crosses.

with the model having δD values less depleted than the in situ data (Figures 9c and 9e). Better agreement at the top of the TTL is achieved by the model, with the best agreement occurring on August 6th (Figure 9a). On all three days a few trajectories do not intersect convection (blue dots). While the effect on the water vapor mixing ratio is apparently small, the effect on the δD value is larger with the trajectories that encountered no convection having δD values 100 to 200‰ lower (i.e. more depleted).

[26] While the results presented in Figure 9 clearly show that using the past 20 day temperature history along with a model of convective influence can accurately reproduce the water vapor and δD profiles observed during TC4 in the TTL, it does not demonstrate whether convection was a necessary component and whether the effect of convection was to increase the water vapor mixing ratio or simply alter the ratio of isotopologues. To quantitatively evaluate the effect of convection on the water vapor mixing ratio, we turn off convection in our model and look at the water vapor profile when only temperature is used to determine it (Figure 10). Note that we still include the δD offset due to convection prior to the start of the trajectories. As expected with no additional input to enrich δD, the modeled δD profiles fall off with altitude to a minimum of around −800‰ on both August 8th and 9th (Figures 10c and 10e). The model results from August 6th are less affected by the lack of convection, possibly indicating that convection older than 20 days was more important in setting the δD for these data. The water vapor results through most of the TTL are mostly invariant regardless of convective influence, but in the upper part of the TTL (above 375 K) the water vapor

profiles that include convection (Figure 9) are noticeably wetter than those that do not include convection (Figure 10). This is most obvious on August 6th (compare Figures 9b and 10b).

[27] To quantify the importance of including recent convection in reproducing the in situ data we plot the fractional difference between the model results and the in situ data for both the model with convection and the model without convection for water vapor (Figures 11a, 11d, and 11g) and for δD (Figures 11b, 11e, and 11h). As qualitatively discussed by comparing Figures 9 and 10 the addition of convection makes a larger difference for δD than for water vapor. On August 8th and 9th the model with convection (red trace) is in closer agreement with the in situ δD data, having a fractional difference near 0, than the model without convection (blue trace). On August 6th, as noted previously, the addition of convection makes little difference for the level of agreement with the in situ data. The opposite is true with respect to water vapor. With the exception of a few data points on August 6th (Figure 11a), the agreement between either model and the in situ data is the same. However, even though the mean fractional change is small there is still a net addition of water to the TTL from convection. We evaluate this addition by taking the difference between the modeled water vapor mixing ratios with and without convective influence (Figures 11c, 11f, and 11i). The difference corresponds to the amount of water vapor added by convection for each trajectory. At the base of the TTL all three days show some enhancements of on average between 0.2 and 1 ppmv. On August 9th (Figure 11i) the enhancements are contained below a θ of 365 K. On both August 6th and 8th convection added on average between 1 and 2 ppmv of water vapor to the top of the TTL ($\theta > 375$ K).
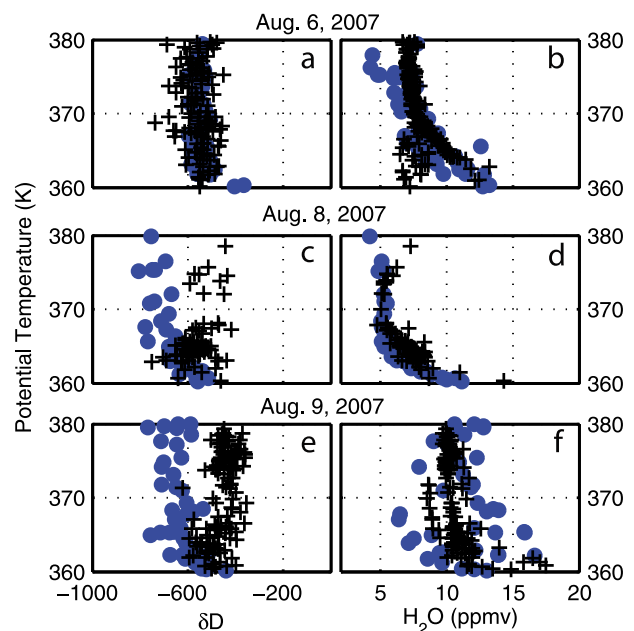

Figure 10. Same as in Figure 9 except model does not include the effect of convection. Only the temperature along each trajectory is used to determine the final mixing ratio and δD.
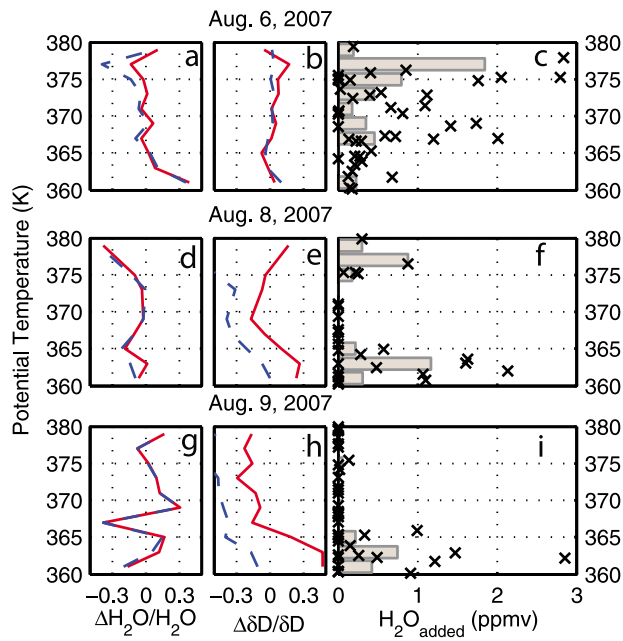
Figure 11. Fractional difference between in situ data and model results including convective influence (red line) and not including convective influence (blue dashed-line) for (a, d, g) water vapor and (b, e, h) δD. (c, f, i) Also shown is the absolute difference in water vapor mixing ratio between model results that include convective influence (as in Figure 9) and model results that do not include convective influence (as in Figure 10). Differences for each trajectory from TC4 are plotted versus potential temperature as black crosses. The mean addition of water vapor binned every 2 K in potential temperature are shown as gray bars.

[28] The convective influence model shows that nearly all the trajectories during TC4 encountered convection in the previous 20 days. However, convection occurring at the beginning of the trajectories had little effect of the final water vapor mixing ratio as the air parcels went through their minimum temperature after the convection. Even so, 60% of the trajectories in the TTL and 55% of the trajectories above 375 K still retained some amount of water vapor added by convection at the end of the 20 day trajectories.

8. Model Results From CR-AVE

[29] We performed similar comparisons for the data from CR-AVE the results of which are shown in Figures 12, 13, and 14. As in TC4 we find that most of the trajectories were influenced by convection in the past 20 days, though a higher proportion saw no convection (blue points in Figure 12). These points have δD values of around $-800‰$, more depleted than any of the in situ data. In addition, on February 1st and 2nd (Figures 12d and 12f) the model under-predicts the amount of water vapor, which may indicate either missed convection or higher supersaturation both of which are supported by the modeled δD being depleted as compared to the in situ data. Qualitatively the model does show an increase in δD above 370 K as in the in situ data. On February 1st and 2nd when the trend to more enriched δD is most pronounced in the in situ data the model

shows enriched values while water vapor is still decreasing. This is compared to January 30th and February 7th when the model shows more depleted values as does the in situ data. However, quantitatively the model under-predicts the increase in δD. In general the agreement during CR-AVE between the model results and the in situ data is not as robust as for the TC4 data. Comparing the model results with and without convection (Figures 12 and 13) we see the same differences as in TC4. The δD results only agree with the in situ data if convection is included in the model. The water vapor shows little difference and as the convection in CR-AVE is almost entirely at the beginning of the trajectories this is not surprising. Quantitatively comparing the water added by convection we find on average 0.5 ppmv of water added at the base of the TTL, with the exception of January 30 (Figure 14c). Through out the rest of the TTL there is almost no net addition of water vapor with the additions being between 0 and 0.2 ppmv. In total 30% of the trajectories in the TTL had some positive, though small, addition of water due to convection during the previous 20 days.

9. Conclusions

[30] We have presented the first in situ measurements of δD in the tropics during summertime and wintertime. This

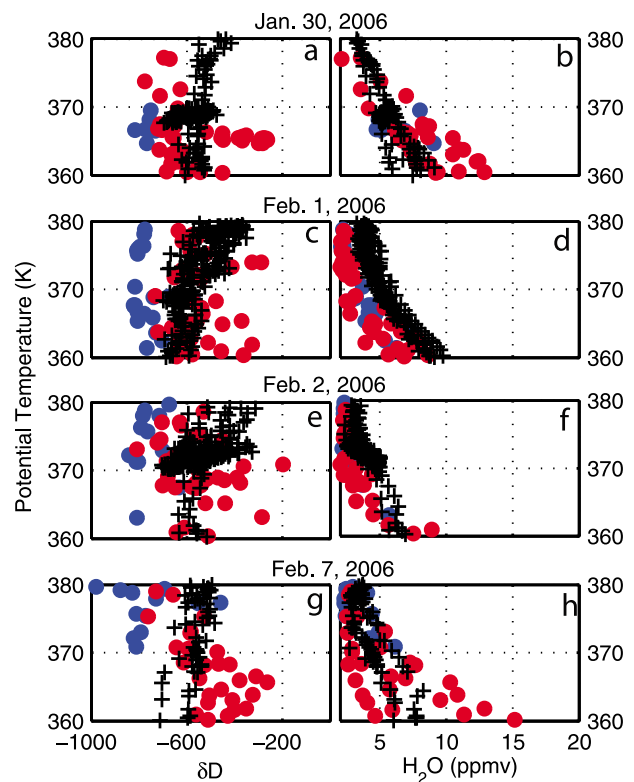**Figure 12.** Comparison of model results and in situ data from CR-AVE. Calculated and measured (a, c, e, g) δD and (b, d, f, h) water vapor are plotted versus potential temperature. Model results are plotted in blue and red for trajectories that were influenced by convection and those that were not influenced by convection in the past 20 days. The measured mixing ratios and δD are shown as black crosses.
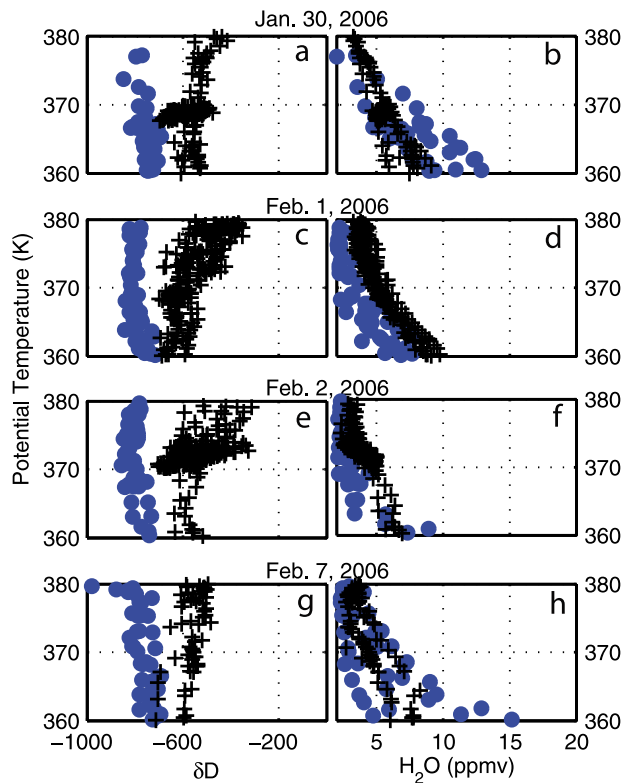
Figure 13. Same as in Figure 9 except model does not include the effect of convection. Only the temperature along each trajectory is used to determine the final mixing ratio and δD.

represents a unique data set to test models of dehydration and convective influence in the TTL. As expected, in situ profiles of δD measured in the tropics during both summertime and wintertime show enrichment compared to if water vapor mixing ratio was controlled solely by minimum temperature. The wintertime measurements have a minimum δD of $-650‰$ at the base of the TTL and are then constant up to 370 K. At the top of the TTL and through the lower tropical stratosphere there is an increase in δD to $-500‰$ accompanied by a small increase in water vapor mixing ratio. Back trajectory models show this enhancement linked to deep convection over South America and the Southern Pacific Ocean.

[31] The summertime data show enriched air starting at the base of the TTL and a uniform δD value throughout the TTL and stratosphere with flight to flight variations ranging from $-450‰$ to $-600‰$ with instrumental uncertainties (30 sec., $1\ \sigma$) of $\pm 17‰$ and $\pm 50‰$ for CR-AVE and TC4, respectively. Water vapor data show similar variations in mixing ratio with the wetter profiles corresponding the isotopically heavier data. In both TC4 and CR-AVE the range of δD values is small with measurements neither showing very enhanced ($\delta D > -200‰$) nor very depleted ($\delta D < -800‰$) air parcels. While this is in agreement with observations from remote sensing instruments, those instruments average over large spatial areas, which would lead to the profiles representing the average δD value. Even with the high spatial and temporal in situ data the TTL

region is fairly homogeneous with all data showing enrichment due to convection.

[32] We use a simple scheme of convective ice evaporation to model the effect of convection on trajectories in the TTL. Dessler07 used this scheme with climatological data to show that by averaging over many trajectories, convection can be used to explain the enhancements in δD observed by remote sensing instruments. Here we have applied that idea to a very detailed case study using the data from TC4 and CR-AVE to demonstrate that minimum temperatures along with a representation of evaporated ice can qualitatively and quantitatively reproduce the in situ data.

[33] The model shows that almost all trajectories both in winter and summer encountered convection in the previous 20 days. 60% of the summer and 30% of the winter trajectories having a net positive addition of water vapor due to convection. During the wintertime the convection mostly occurred early in the trajectories and therefore the net change in water vapor was on average less than 0.2 ppmv. For the summertime data more recent convection produced
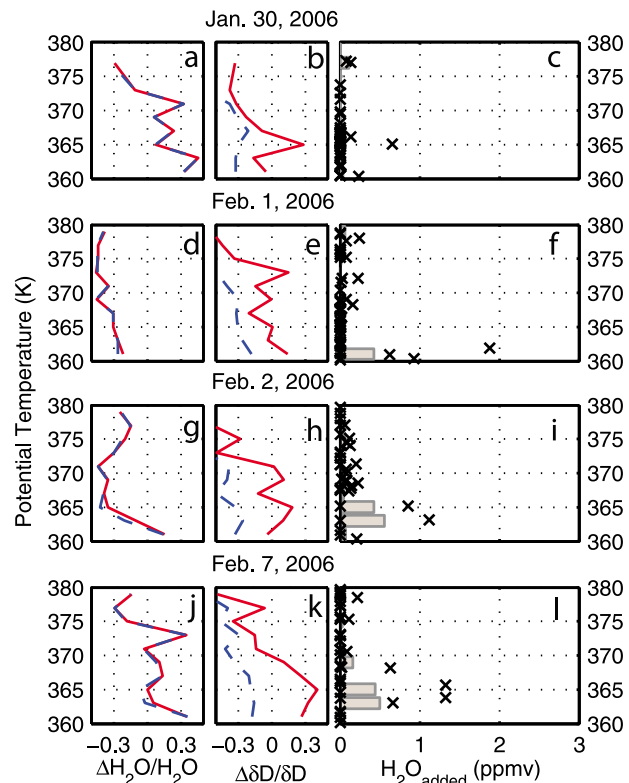

Figure 14. Fractional difference between in situ data and model results including convective influence (red line) and not including convective influence (blue dashed-line) for (a, d, g, j) water vapor and (b, e, h, k) δD. (c, f, i, l) Also shown is the absolute difference in water vapor mixing ratio between model results that include convective influence (as in Figure 12) and model results that do not include convective influence (as in Figure 13). Differences for each trajectory from CR-AVE are plotted versus potential temperature as black crosses. The mean addition of water vapor binned every 2 K in potential temperature is shown as gray bars.

enhancements of up to 2 ppmv at the top of the TTL ($\theta > 375$ K).

[34] In winter convection occurred mainly over the Western Tropical Pacific and South America with some convection also over Africa and the Southern Pacific Ocean. Most convection was below 365 K, with the exception of the convection over South America that reached potential temperatures above 390 K. This deep convection is collocated with the air sampled above 370 K and explains the shift in δD values at this altitude. Summertime convection occurred over Asia, Africa, and South America in the tropics and air from the North American monsoon was also sampled with convection occurring over North America.

[35] The data and model results presented here demonstrate that water vapor mixing ratio is mainly controlled by minimum temperature history and the δD values are mainly set by the history of convective encounters. This is in agreement with the conclusions of Dessler07 and others who show that addition of convective ice can explain δD with only a small perturbation to water vapor. Here we have quantified that addition of water vapor and show that, though small, convection still has a positive influence on the water vapor mixing ratio. During the wintertime the addition on average is less than 0.2 ppmv throughout most of the TTL and up to 0.5 ppmv at the base of the TTL. During the summertime the addition of water vapor by convection is variable with some days showing almost no increase in water vapor by convection. On other days convection is more significant with mean additions of 1 to 2 ppmv at the top of the TTL which accounts for between 20 and 30% of the water vapor measured.

[36] Measurements of δD can be used to effectively constrain the amount of convective ice that needs to be added to models and are necessary to include in models to accurately predict the amount of water vapor in the TTL and entering the tropical stratosphere. The data presented here were limited to near Costa Rica. To further quantify the amount of water vapor added by convection a more detailed sampling of the tropics needs to occur with measurements especially in the other convectively active regions. In addition, sampling of convective outflow and measurements of the δD of ice at various altitudes is necessary to understand the variability in the δD of ice which would allow for better constraints on the model.

References

Bloom, S., A. da Silva, D. Dee, M. Bosilovich, J. Chern, S. Pawson, S. Schubert, M. Sienkiewicz, I. Stajner, W. Tan, and M. Wu (2005), Documentation and validation of the Goddard Earth Observing System (GEOS) data assimilation system - version 4, *NASA Tech. Memo., TM-104606*, vol. 26, 161 pp.

Bony, S., C. Risi, and F. Vimeux (2008), Influence of convective processes on the isotopic composition (δ^{18}O and δD) of precipitation and water vapor in the tropics: 1. Radiative-convective equilibrium and Tropical Ocean-Global Atmosphere-Coupled Ocean-Atmosphere Response Experiment (TOGA-COARE) simulations, *J. Geophys. Res., 113*, D19305, doi:10.1029/2008JD009942.

Cau, P., J. Methven, and B. Hoskins (2007), Origins of dry air in the tropics and subtropics, *J. Clim., 20*(12), 2745–2759, doi:10.1175/JCLI4176.1.

Corti, T., et al. (2008), Unprecedented evidence for deep convection hydrating the tropical stratosphere, *Geophys. Res. Lett., 35*, L10810, doi:10.1029/2008GL033641.

Craig, H. (1961a), Standard for reporting concentrations of deuterium and oxygen-18 in natural waters, *Science, 133*, 1833–1834. doi:10.1126/science.133.3467.1833.

Craig, H. (1961b), Isotopic variations in meteoric waters, *Science, 133*, 1702–1703, doi:10.1126/science.133.3465.1702.

Dessler, A. E., T. F. Hanisco, and S. Fueglistaler (2007), Effects of convective ice lofting on H_2O and HDO in the tropical tropopause layer, *J. Geophys. Res., 112*, D18309, doi:10.1029/2007JD008609.

Dvortsov, V. L., and S. Solomon (2001), Response of the stratospheric temperatures and ozone to past and future increases in stratospheric humidity, *J. Geophys. Res., 106*, 7505–7514.

Ehhalt, D., F. Rohrer, and A. Fried (2005), Vertical profiles of HDO/H_2O in the troposphere, *J. Geophys. Res., 110*, D13301, doi:10.1029/2004JD005569.

Fasullo, J., and D. Z. Sun (2001), Radiative sensitivity to water vapor under all-sky conditions, *J. Clim., 14*, 2798–2807.

Fu, R., Y. L. Hu, J. S. Wright, J. H. Jiang, R. E. Dickinson, M. X. Chen, M. Filipiak, W. G. Read, J. W. Waters, and D. L. Wu (2006), Short circuit of water vapor and polluted air to the global stratosphere by convective transport over the tibetan plateau, *Proc. Natl. Acad. Sci. U. S. A., 103*, 5664–5669.

Fueglistaler, S., H. Wernli, and T. Peter (2004), Tropical troposphere-to-stratosphere transport inferred from trajectory calculations, *J. Geophys. Res., 109*, D03108, doi:10.1029/2003JD004069.

Fueglistaler, S., M. Bonazzola, P. H. Haynes, and T. Peter (2005), Stratospheric water vapor predicted from the lagrangian temperature history of air entering the stratosphere in the tropics, *J. Geophys. Res., 110*, D08107, doi:10.1029/2004JD005516.

Gulstad, L., and I. S. A. Isaksen (2007), Modeling water vapor in the upper troposphere and lower stratosphere, *Terr. Atmos. Oceanic Sci., 18*(3), 415–436, doi:10.3319/TAO.2007.18.3.415.

Hanisco, T. F., et al. (2007), Observations of deep convective influence on stratospheric water vapor and its isotopic composition, *Geophys. Res. Lett., 34*, L04814, doi:10.1029/2006GL027899.

Holton, J. R., and A. Gettelman (2001), Horizontal transport and the dehydration of the stratosphere, *Geophys. Res. Lett., 28*, 2799–2802.

Holton, J. R., P. H. Haynes, M. E. McIntyre, A. R. Douglass, R. B. Rood, and L. Pfister (1995), Stratosphere-troposphere exchange, *Rev. Geophys., 33*, 403–439.

James, R., and B. Legras (2009), Mixing processes and exchanges in the tropical and the subtropical UT/LS, *Atmos. Chem. Phys., 9*(1), 25–38.

Jensen, E., and L. Pfister (2005), Implications of persistent ice supersaturation in cold cirrus for stratospheric water vapor, *Geophys. Res. Lett., 32*, L01808, doi:10.1029/2004GL021125.

Jensen, E. J., et al. (2005), Ice supersaturations exceeding 100% at the cold tropical tropopause: Implications for cirrus formation and dehydration, *Atmos. Chem. Phys., 5*, 851–862.

Johnson, D. G., K. W. Jucks, W. A. Traub, and K. V. Chance (2001), Isotopic composition of stratospheric water vapor: Implications for transport, *J. Geophys. Res., 106*, 12,219–12,226.

Jouzel, J., L. Merlivat, and B. Federer (1985), Isotopic study of hail—The δd-δ^{18}O relationship and the growth history of large hailstones, *Q. J. R. Meteorol. Soc., 111*, 495–516.

Kalnay, E., et al. (1996), The ncep/ncar 40-year reanalysis project, *Bull. Am. Meteorol. Soc., 77*(3), 437–471.

Keith, D. (2000), Stratosphere-troposphere exchange: Inferences from the isotopic composition of water vapor, *J. Geophys. Res., 105*, 15,167–15,173.

Kelly, K. K., M. H. Proffitt, K. R. Chan, M. Loewenstein, J. R. Podolske, S. E. Strahan, J. C. Wilson, and D. Kley (1993), Water-vapor and cloud water measurements over darwin during the step 1987 tropical mission, *J. Geophys. Res., 98*, 8713–8723.

Kirk-Davidoff, D. B., E. J. Hintsa, J. G. Anderson, and D. W. Keith (1999), The effect of climate change on ozone depletion through changes in stratospheric water vapour, *Nature, 402*, 399–401.

Kuang, Z., G. Toon, P. Wennberg, and Y. Yung (2003), Measured HDO/H_2O ratios across the tropical tropopause, *Geophys. Res. Lett., 30*(7), 1372, doi:10.1029/2003GL017023.

Minschwaner, K., and A. E. Dessler (2004), Water vapor feedback in the tropical upper troposphere: Model results and observations, *J. Clim., 17*, 1272–1282.

Moyer, E., F. Irion, Y. Yung, and M. Gunson (1996), ATMOS stratospheric deuterated water and implications for troposphere-stratosphere transport, *Geophys. Res. Lett., 23*(17), 2385–2388.

Pfister, L., K. R. Chan, T. P. Bui, S. Bowen, M. Legg, B. Gary, K. Kelly, M. Proffitt, and W. Starr (1993), Gravity-waves generated by a tropical cyclone during the step tropical field program: A case-study, *J. Geophys. Res.*, *98*, 8611–8638.

Pfister, L., et al. (2001), Aircraft observations of thin cirrus clouds near the tropical tropopause, *J. Geophys. Res.*, *106*, 9765–9786.

Pfister, L., H. B. Selkirk, D. O. Starr, K. Rosenlof, and P. A. Newman (2010), A meteorological overview of the TC4 mission, *J. Geophys. Res.*, *115*, D00J12, doi:10.1029/2009JD013316.

Pollock, W., L. E. Heidt, R. Lueb, and D. H. Ehhalt (1980), Measurement of stratospheric water-vapor by cryogenic collection, *J. Geophys. Res.*, *85*, 5555–5568.

Rosenfield, J. E. (1991), A simple parameterization of ozone infrared-absorption for atmospheric heating rate calculations, *J. Geophys. Res.*, *96*, 9065–9074.

Sayres, D. S., et al. (2009), A new cavity based absorption instrument for detection of water isotopologues in the upper troposphere and lower stratosphere, *Rev. Sci. Instrum.*, *80*, 044102, doi:10.1063/1.3117349.

Schoeberl, M., and L. C. Sparling (1995), Trajectory modelling, diagnostic tools in atmospheric science, in *Proceedings of the International School of Physics*, edited by G. Fiocco and G. Visconti, pp. 289–305, IOS Press, Amsterdam.

Smith, C. A., J. D. Haigh, and R. Toumi (2001), Radiative forcing due to trends in stratospheric water vapour, *Geophys. Res. Lett.*, *28*, 179–182.

St. Clair, J. M., et al. (2008), A new photolysis laser induced fluorescence technique for the detection of HDO and H_2O in the lower stratosphere, *Rev. Sci. Instrum.*, *79*, 06401, doi:10.1063/1.2940221.

Weinstock, E. M., E. J. Hintsa, A. E. Dessler, J. F. Oliver, N. L. Hazen, J. N. Demusz, N. T. Allen, L. B. Lapson, and J. G. Anderson (1994), New fast-response photofragment fluorescence hygrometer for use on the NASA ER-2 and the Perseus remotely piloted aircraft, *Rev. Sci. Instrum.*, *65*, 3544–3554.

Yang, Q., Q. Fu, and Y. Hu (2010), Radiative impacts of clouds in the tropical tropopause layer, *J. Geophys. Res.*, *115*, D00H12, doi:10.1029/2009JD012393.

J. G. Anderson, A. S. O'Brien, D. S. Sayres, J. B. Smith, and M. F. Witinski, School of Engineering and Applied Sciences, Harvard University, 12 Oxford St., Cambridge, MA 02138, USA. (sayres@huarp.harvard.edu)

T. F. Hanisco, NASA Goddard Space Flight Center, 8800 Greenbelt Rd., Greenbelt, MD 20771, USA.

M. Legg, BAERI, 560 3rd St. W., Sonoma, CA 95476, USA.

E. J. Moyer, Department of Geophysical Sciences, University of Chicago, 5734 S. Ellis Ave., Chicago, IL 60637, USA.

L. Pfister, NASA Ames Research Center, Moffett Field, CA 94035, USA.

J. M. St. Clair, Geology and Planetary Sciences Division, California Institute of Technology, MC 17-25, 1200 E. California Blvd., Pasadena, CA 91125, USA.